Spatio-Temporal Imaging of Ultrafast Molecular Motion: 'Collapse' and Revival of D_2^+ Nuclear Wave Packet

Th. Ergler[1], A. Rudenko[1], B. Feuerstein[1,2], K. Zrost[1,3], C.D. Schröter[1], R. Moshammer[1] and J. Ullrich[1]

[1] *Max-Planck-Institut für Kernphysik, D-69029 Heidelberg, Germany*

[2] *Physikalisches Institut, Universität Heidelberg, 69120 Heidelberg, Germany*

[3] *Research School of Physical Sciences and Engineering, The Australian National University, ACT 0200, Australia*

We report on a real-time imaging of the ultrafast D_2^+ ro-vibrational nuclear wave-packet motion performed using a combination of a pump-probe setup with 7 fs laser pulses and a "reaction microscope" spectrometer. We observe fast dephasing ("collapse") of the vibrational wave packet and its subsequent revival, and prove rotational excitation in ultrashort laser pulses. Channel-selective Fourier analysis of the wave packet's long-term (~ 3000 fs) evolution allows us to resolve its individual constituents, revealing unique information on the mechanisms of strong-field ionization and dissociation.

33.80.Rv, 32.80.Rm, 42.50.Hz

Pump-probe experiments employing femtosecond laser pulses in combination with rapidly developing few-particle imaging techniques allow one to get a deeper insight into quantum dynamics of nuclear motion in bound molecules and molecular reactions [1]. For different molecular systems the formation and time evolution of dissociating (see e.g., [2]), rotational [3] and vibrational [4] wave packets have been investigated, and, under certain conditions, images of the squared nuclear wave function have become accessible [2,4]. Yet, the simplest of all molecules, the hydrogen (deuterium) molecular ion, which represents fundamental test grounds for advancing molecular quantum theory and a model laboratory system for studies of laser-molecule interactions [5], has essentially resisted numerous attempts to comprehensively explore its nuclear motion. For these most fundamental molecular systems vibrational dynamics proceed on the 10 fs scale, which is still well below the 25 fs laser pulses of "ultrashort" commercial systems. As a consequence, time-resolved studies of hydrogen (deuterium) nuclear wave packets were practically restricted to their dissociating (continuum) part [6-8].

In order to trace the wave-packet's motion in the bound-state a novel approach known as the 'molecular clock' scheme, where the electrons ionized via tunneling and driven back to the parent ion by the oscillating laser field are used as an ultrafast probe, either observing "recollision"-induced electron-impact fragmentation [9-10], or high-harmonic radiation [11], has been developed. Though providing superior sub-fs time-resolution, this technique is (i) intrinsically restricted to fixed return times given by the laser frequency, (ii) by definition explores the molecular motion in the presence of a strong disturbing field and (iii) cannot be used to study the long-time propagation of the wave packet. Therefore, considerable efforts are presently being undertaken to realize "classical" pump-probe experiments with sub-10 fs time resolution, and very recently clear signatures of the bound-state vibrational motion have been observed [12-15].

In this Letter we report on the high-resolution real-time mapping of D_2^+ nuclear wave packets using time-resolved three-dimensional Coulomb explosion (CE) imaging [16]. We

observe a good agreement with the results of numerical simulations of the wave packet propagation [17], and provide experimental evidence for rotational excitation even in ultrashort few-cycle laser pulses. In contrast to previous time-resolved studies on H_2 (D_2), we visualize the spatio-temporal structure of both vibrational and rotational wave packets within one measurement, and trace its long-term (up to ~ 3000 fs), almost field-free evolution, which allows us to resolve individual vibrational states contributing to the wave packet formation via channel-selective Fourier analysis. The latter results provide benchmark data for theoretical analyses of the ionic wave packet generated by ionization of a neutral molecule in intense ultrashort laser fields, as well as of dissociation mechanisms.

As illustrated in Fig. 1, we prepare a coherent superposition of the D_2^+ ro-vibrational states via tunnelling ionization of the neutral D_2 molecule in its ground state by an intense ($5*10^{14}$ W/cm^2) linearly polarized 7 fs laser pulse. Created molecular ions either dissociate along the field modified $2p\sigma_u$ potential curve or remain bound in the $1s\sigma_g$ potential. Both, continuum and bound parts of the wave packet are then projected onto the repulsive Coulomb curve by ionizing the D_2^+ ions with a more intense (10^{15} W/cm^2) probe pulse arriving after a certain time delay and, thus, 'exploding' the molecule. The measured energy release consists of the Coulomb energy and the kinetic energy at the moment of explosion. Since for the bound wave packet the latter component is rather small, the internuclear distance R can be directly reconstructed from the measured deuteron energy using the Coulomb law. Simultaneous determination of the emission angle with respect to the direction of the laser polarization (see Fig. 1) yields the information on the orientation of the internuclear axis at the moment of explosion. Due to the cylindrical symmetry of the problem with respect to the laser polarization axis, these two observables contain complete three-dimensional information on the probability density distribution of the nuclear wave packet.

Measurements were performed using an experimental set up described in [8,15,18]. We used 7 fs (FWHM) linearly polarized pulses with a center wave length of ~ 760 nm. The laser

beam was fed through a Mach-Zehnder type interferometer with one arm variable in length, providing two pulses separated by a time delay which can be scanned from 0 to 3.3 ps with a resolution of better than 0.3 fs. By measuring the autocorrelation directly at the reaction volume using the ion rate as non-linear signal we verify *in situ* the length of the pulse and the absolute time zero of the delay. Both laser beams were focused to a spot size of ~ 5 μm onto a supersonic molecular gas jet in the center of an ultra-high vacuum chamber (2×10^{-11} mbar). Charged reaction fragments were guided onto two position-sensitive channel plate detectors by weak electric (2 V/cm) and magnetic (7 G) fields applied along the laser polarization axis. From the time-of-flight and position on the detectors the full momentum vectors of the coincident recoil ions and electrons were calculated. By inspecting momentum conservation for multi-photon single ionization, the internal temperature of the jet was determined to be about 3 K such that D_2 molecules are well prepared in their ground state.

Fig. 2a displays the experimental D^+ kinetic energy spectrum as a function of the time delay between the pump and the probe pulses, integrated over all D^+ emission angles. Three major contributions can be distinguished. First, a broad clearly structured and well-resolved band centred at ~ 4 eV can be observed *(pathway 1)* over the whole range of delays resulting from CE of the rotating and vibrating D_2^+ molecule. Second, a pronounced descending line can be distinguished *(pathway 2)* reflecting D_2^+ molecules dissociating after the pump and exploded by the probe pulse [7,8,12,15]. Finally, there is an intense dissociation band at 0 - 1 eV kinetic energy *(pathway 3),* where the molecule is dissociated either by the pump or the probe.

Exploiting CE imaging we now plot the nuclear wave-packet probability density as a function of the internuclear distances R (Fig. 2b) and compare the result with theoretical simulations (Fig. 2c) assuming an instant vertical Franck-Condon transition from the ground state of D_2 (for details of the calculation see [17]). The pump-pulse induced dissociating part (*pathway* 2) is reflected by a fast ascending line propagating beyond R ~ 5 Å in less than 100 fs. The bound-state part (*pathway 1*) appears as a broad structure spreading up to R ~ 4 Å in the

experiment and even 5 Å in the simulation, demonstrating that we are indeed able to image the wave-packet at any time and at practically all internuclear distances. Differences in the R-dependent intensity between experiment and simulation are most likely due to deficiencies of our simple model, which does not account for the R-dependence of D_2^+ ionization probability [19,20] and assumes a Frank-Condon transition for the wave packet preparation.

For delays up to 100 fs a series of well-resolved stripes separated by ~ 24 fs (descending in energy and ascending in R representation) can be observed in both, the experimental data and the simulations, reflecting the vibrational motion of the bound D_2^+. In striking contrast with the classical idea of the two-centre molecule oscillating back and forth, the wave packet exhibits a noticeable localization only on its way out, experimentally as well as theoretically. Being of purely quantum-mechanical nature, this behaviour in an oversimplified picture can be considered as a consequence of positive or negative dispersion experienced by the wave packet during its reflection from the outer and inner turning points, respectively. This leads to the wave packet spreading at the outer turning point and its partial recompression at the inner one [21].

Already after few oscillations, the anharmonicity of the potential curve, i.e., the non-equal spacing of the vibrational levels populated by the pump pulse, leads to the dephasing, or 'collapse' of the wave packet, reflected in the apparent degeneration of the vibrational structures for delays close to 100 fs. However, after about 500 fs the stripes reappear, indicating a restored periodicity of the wave packet motion. This phenomenon is known as a quantum wave packet revival (see [22] for reviews) and arises in weakly anharmonic systems with a long-time preserved coherence. Whereas the phenomenon of revivals has been extensively investigated in the time domain for various atomic, molecular and optical systems, the present study, represents, to the best of our knowledge, the first example for the observation of the revival structure resolved in both *time* and *space* (i.e., in internuclear distance).

In both, the experimental data and the simulation an additional structure with ~ 12 fs periodicity can be observed at 200-300 fs, reflecting a so-called fractional revival. Here, the

wave packet consists essentially of two copies of the initial one, each shifted against the other by half of the vibrational period [22]. Dynamical interference between these two "counter-propagating" waves produces a periodic pattern at a frequency doubled compared to the fundamental vibrational one [4,22], representing an impressive example of the wave-like nature of the nuclear motion in molecules.

Having visualized the vibrational motion of the D_2^+ wave packet, we now turn our attention to the rotation of the molecule. For the case of H_2 / H_2^+ despite numerous experimental and theoretical studies, the issue concerning its rotational excitation is still obscure, and so far no direct experimental evidence for dynamic alignment of H_2^+ in fs laser pulses exists (see [23] and references therein for a detailed discussion). Moreover, whereas it was recently shown that a linearly polarized laser pulse considerably shorter than the rotational period can excite a coherent superposition of rotational states, inducing post-pulse field-free dynamic alignment [3], these effects until now have not been observed with few-cycle pulses for any molecular system. In order to clarify, whether in the present experiment the ultrashort 7 fs pump pulse excites a rotational wave packet, in Fig. 3 b-d we have plotted the time-dependent CE rate (in the energy range between 3 and 4 eV) for various angular intervals $\Delta\theta_i$ of the exploding molecule with respect to the laser polarization direction $\hat{\varepsilon}$ (as illustrated in Fig. 1b). For comparison, the corresponding D^+ rate integrated over all θ is displayed as well (Fig. 3a). Evident differences between spectra with varying $\Delta\theta_i$ are found, most strikingly around the vibrational revival times. Whereas here the data e.g. for $\Delta\theta_1 = (0\text{-}10)°$ exhibit a clear dip, spectra for $\Delta\theta_2 = (20\text{-}30)°$ display a maximum which is shifted towards larger delays for $\Delta\theta_3 = (40\text{-}50)°$. Thus, we undoubtedly observe signatures of D_2^+ rotational motion (i.e., dynamical alignment [23]) and proof that it can be induced even by an ultrashort 7 fs laser pulse. A more detailed analysis of the rotational wave packet taking into account θ-dependence of the D_2^+ ionization probability for linearly polarized pulses [19] will be presented elsewhere.

Detailed quantitative information about the wave packet structure in the frequency domain can be obtained by a Fourier analysis of its time evolution. This is especially interesting since there exist numerous theoretical studies investigating the dissociation dynamics and predicting the distribution of H_2^+ (D_2^+) vibrational states produced by strong-field ionization of H_2 (D_2) [5,24], with only one experimental work directly measuring this distribution (for 45 fs pulses) being at hand [25]. In Fig. 4 we present the Fourier-analysis result of the bound-state D_2^+ wave packet motion in different CE energy windows as well as of the dissociation channel. An extended time-delay range up to 3000 fs was realized in order to achieve sub meV resolution.

Several important results are obtained: First, we find that the frequencies *f* obtained for the individual vibrational transitions $f(v_{ij})$ are in excellent agreement with known spectroscopic data [26] (thin lines in Fig. 4) for practically all states identified demonstrating the high-resolution capabilities of our experimental set-up. Second, distinct systematic differences in the wave-packet composition are obvious while probing it at different CE energies and, thus, at different R with higher vibrational states reaching out to larger internuclear distances as expected. Third, apart from the CE imaging, the D_2^+ wave packet can be probed via dissociating it by the second pulse. This probing channel provides unique information on the distribution of the vibrational states involved in the dissociation by intense ultrashort laser pulses (Fig 4e). Surprisingly, the main part of the distribution contains the vibrational states below the border for the one-photon transition ($v \geq 7$) [26], which, from the measured fragment energy spectra, is expected to dominate for the ultrashort pulses [18]. The observed distribution is very similar to that obtained by CE at 3.5-4 eV (Fig. 4b) indicating that the dissociation essentially occurs at the internuclear distances of 1.8-2.1 Å, which is consistent with the (resonant) three-photon transition from the $1s\sigma_g$ to the $2p\sigma_u$ potential curve [5] (see Fig. 1b).

In conclusion, we have mapped in space and time the ro-vibrational motion of D_2^+ bound-state and dissociating wave packets using 7 fs pump-probe pulses with 0.3 fs time-step resolution in combination with an advanced "reaction-microscope" three-dimensional imaging

spectrometer. We provide high-resolution data for the simplest and fastest (apart from H_2/H_2^+) molecular system helping to advance strong-field theory and find unambiguous signatures of D_2^+ rotational excitation in a few cycle pulses. In good agreement with earlier theoretical predictions [17] we are able to visualize a fast dephasing ("collapse") of the vibrational wave packet and its subsequent fractional or nearly complete reconstruction (revival). By following the ro-vibrational motion for time periods as long as 3 ps, enabling high-resolution Fourier analysis of the wave packet motion, channel-selective decomposition of contributing individual vibrational states became possible yielding unprecedented detailed information on the wave packet generation. Moreover, as illustrated in the inset of Fig. 4e, the same Fourier spectra provide information about the composition of the rotational wave packet.

Tracing wave packets for time-intervals up to nanoseconds along with the possibility to obtain the absolute time scale by locking the pulses with the frequency comb technique points to the possibility to perform precision spectroscopy in the time domain with 10^{-7} eV ($\sim 10^{-3}$ cm^{-1}) resolution, challenging conventional techniques. Furthermore, following the ro-vibrational motion (in particular, revival structures) over such long time scales will provide direct information on decoherence times and mechanisms (e.g., ro-vibrational coupling [27] or interaction with the environment) in molecular systems. Finally, the demonstrated possibility to diagnose in details the spatio-temporal structure as well as the spectral composition of an ultrafast molecular wave packet, along with the recent developments in adaptive pulse-shaping techniques represents an important advance in the arising field of wave packet engineering and strong-field coherent control.

1. For a recent review see I.V. Hertel, and W. Radloff, *Rep. Prog. Phys*. **69** 1897 (2006).

2. E. Skovsen *et. al., Phys. Rev. Lett.* **89** 133004 (2002).

3. I.V. Litvinyuk *et. al.*, *Phys. Rev. Lett*., **90** 233003 (2003).

4. H. Katsuki *et. al.*, *Science* **311** 589 (2006).

5. J.H. Posthumus, *Rep. Prog. Phys.* **67** 623 (2004).

6. J.H. Posthumus, *et al*. *J. Phys. B* **32** L93 (1999).

7. C. Trump, H. Rottke, and W. Sandner, *Phys. Rev. A* **59** 2858 (1999).

8. Th. Ergler *et. al., Phys. Rev. Lett.* **95** 093001 (2005).

9. H.Niikura *et al., Nature* **417** 917 (2002); **421** 826 (2003).

10. A.S. Alnaser *et al., Phys. Rev. Lett*. **93** 183202 (2004).

11. S. Baker, *et al., Science* **312** 424 (2006).

12. A.S. Alnaser *et al., Phys. Rev. A* **72** 030702 (R) (2005).

13. F. Légaré *et. al*., *Phys. Rev. A* **72** 052717 (2005).

14. H. Niikura, D.M. Villeneuve, and P.B. Corkum, *Phys. Rev. A* **73** 021402 (R) (2006).

15. Th. Ergler *et. al*., *J. Phys. B* **39** S493 (2006).

16. S. Chelkowski, P.B. Corkum and A.D. Bandrauk, *Phys. Rev. Lett.* **82** 3416 (1999).

17. B. Feuerstein and U. Thumm, *Phys Rev. A* **67** 063408 (2003).

18. A. Rudenko *et. al*., *J. Phys. B* **38** 487 (2005).

19. X.M. Tong, Z.X. Zhao, and C.D. Lin, *Phys Rev. A* **66** 033402 (2002).

20. T. Zuo and A.D. Bandrauk, *Phys. Rev. A* **52** R2511 (1995).

21. X.N. Tong and C.D. Lin, *Phys. Rev. A* **73** 042716 (2006).

22. I.Sh. Averbuch and N.F. Perelman, *Sov. Phys. Usp*. **34** 572 (1991); R.W. Robinet, *Phys. Rep*. **392** 1 (2004).

23. M. Uhlmann, T. Kunert, and R. Schmidt, *Phys Rev. A* **72** 045402 (2005).

24. T.K. Kjeldsen, and L.B. Madsen, *Phys. Rev. Lett*. **95** 073004 (2005).

25. X. Urbain, *et al., Phys. Rev. Lett*. 92 (2004) 163004.

26. G. Hunter, A.W. Yau, and H.O. Pritchard, *Atomic Data and Nuclear Data Tables* **14** 1 (1974).

27. J. Banerji and S. Ghosh, *J. Phys. B,* **39** 1113 (2006).

Figure legends

Figure 1. (a) A scheme of the pump-probe experiment and the relevant potential curves of D_2 and D_2^+. The curves are shown for a field-free situation. The three-photon transition around R ≈ 1.9 Å is indicated by three arrows. (b) Schematic of the experimental geometry. θ denotes the measured D^+ emission angle (and, thus, the orientation of the internuclear axis) relative to the laser polarization direction $\vec{\mathcal{E}}$.

Figure 2. (a) D^+ kinetic energy spectrum as a function of the delay between the pump and the probe pulses. Numbers in the figure indicate the pathways discussed in the text.

(b) The distribution of the D_2^+ wave-packet probability density as a function of the internuclear distances R and the delay between the pump and the probe pulses reconstructed from the experimental data. (c) Calculated density plot of D_2^+ wave packet propagation.

Figure 3. Measured CE yield of the D^+ ions in the 3-4 eV energy interval as a function of the delay τ between the pump and the probe pulses. (a) Integrated over all emission angles θ relative to the laser polarization direction. (b) $0° \le \theta \le 10°$. (c) $20° \le \theta \le 30°$. (d) $40° \le \theta \le 50°$.

Figure 4. Fourier transform of the time-dependent CE yield in the 3-3.5 eV (a), 3.5-4 eV (b), 4-4.5 eV (c), 4.5-5 eV (d) energy intervals, and of the dissociation yield (e). Thin vertical lines show the frequencies of the vibrational transitions known from the spectroscopic data [26]. Numbers on top of the figure indicate the corresponding transitions: The frequency $f((\nu_{i,i+1})$ is denoted by the number *i*. Inset: Fourier transform of the time-dependent dissociation yield for low frequencies. Clear peaks due to the rotational transitions can be observed.

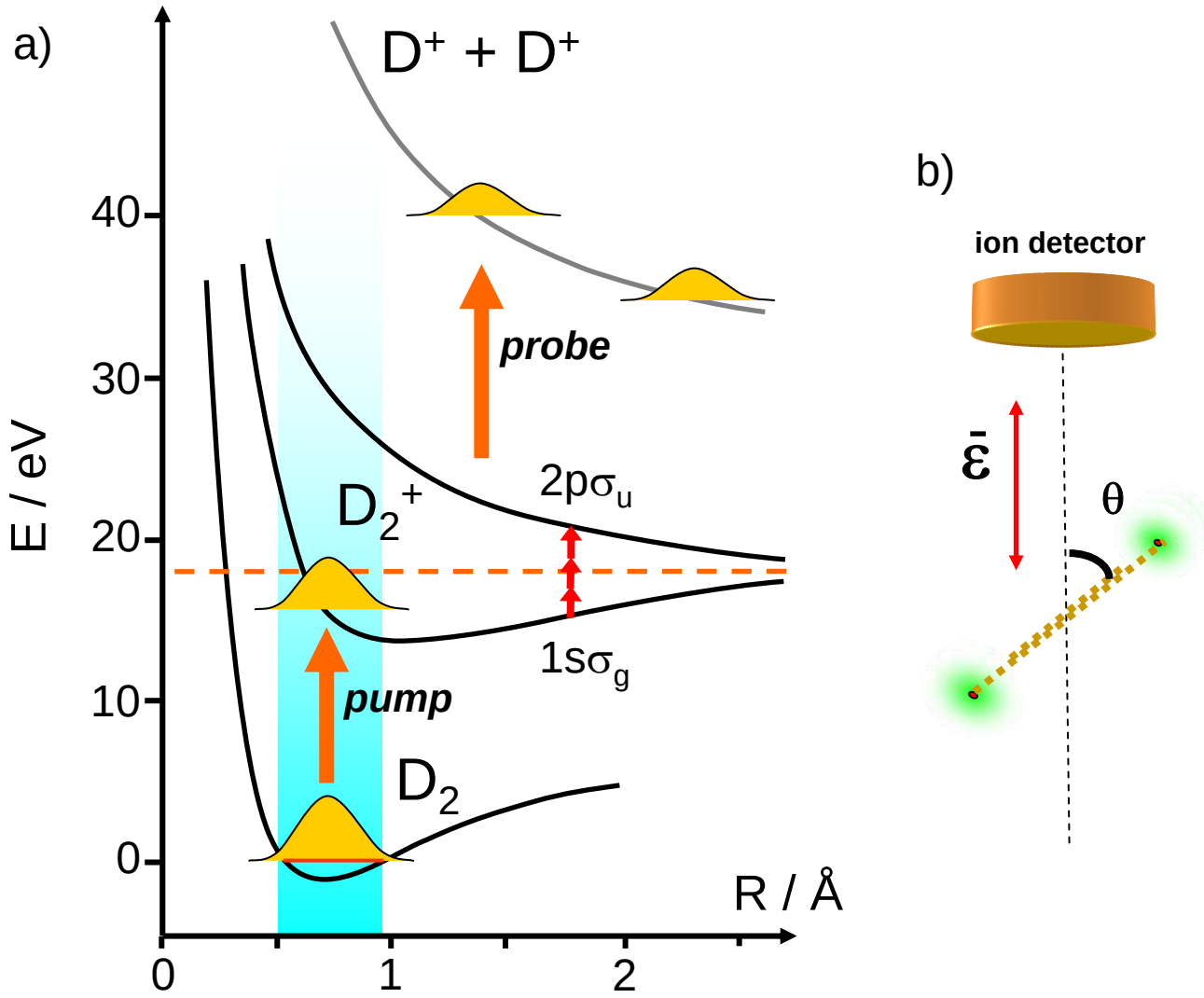
a)
D+ + D+
probe
D2+
2pσu
1sσg
pump
D2
E / eV
R / Å
0
10
20
30
40
0
1
2
b)
ion detector
ε
θ

Figure 1

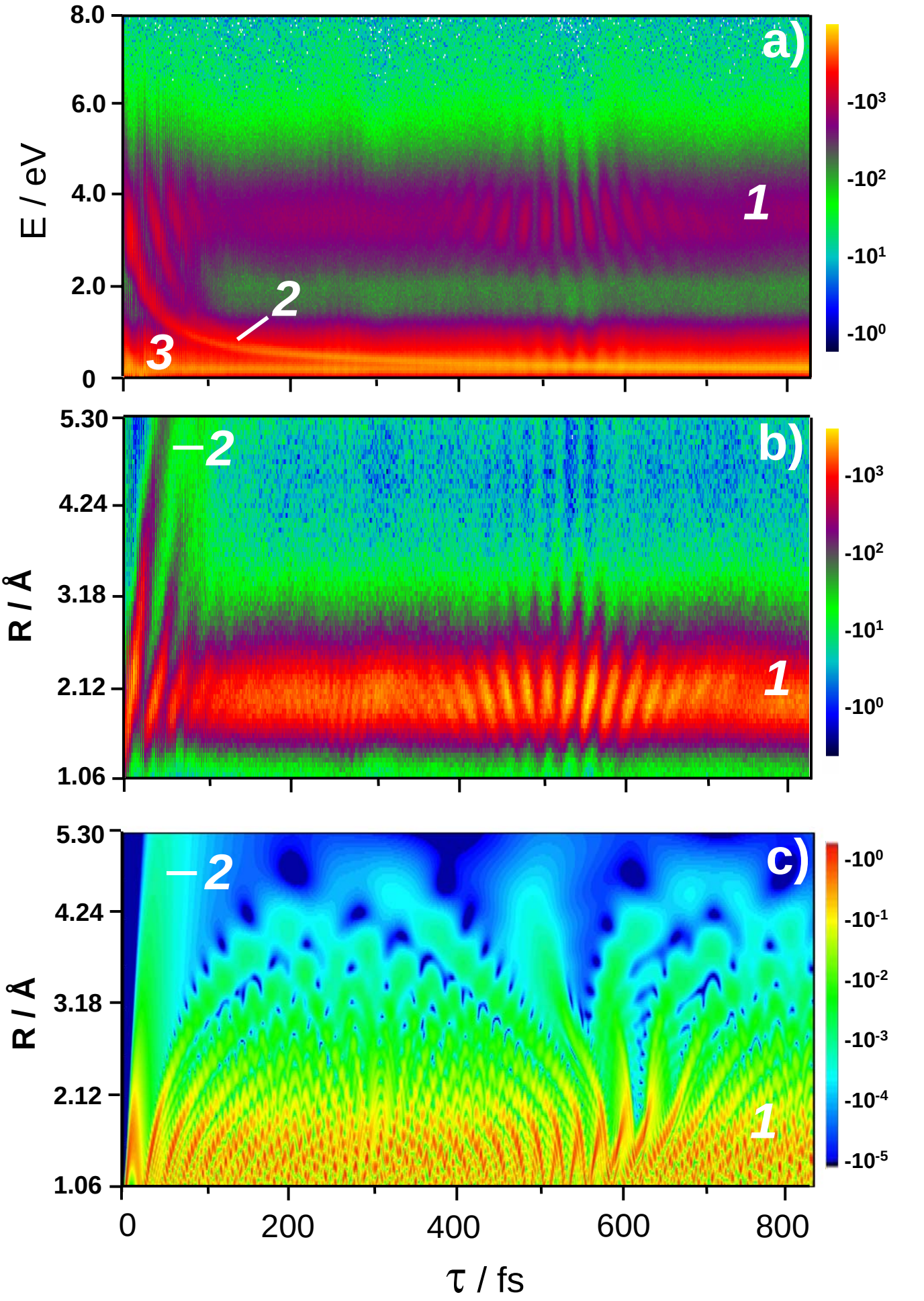
a)
b)
c)
E / eV
R / Å
τ / fs
8.0
6.0
4.0
2.0
0
5.30
4.24
3.18
2.12
1.06
0
200
400
600
800
1
2
3
-10³
-10²
-10¹
-10⁰
-10⁻¹
-10⁻²
-10⁻³
-10⁻⁴
-10⁻⁵

Figure 2

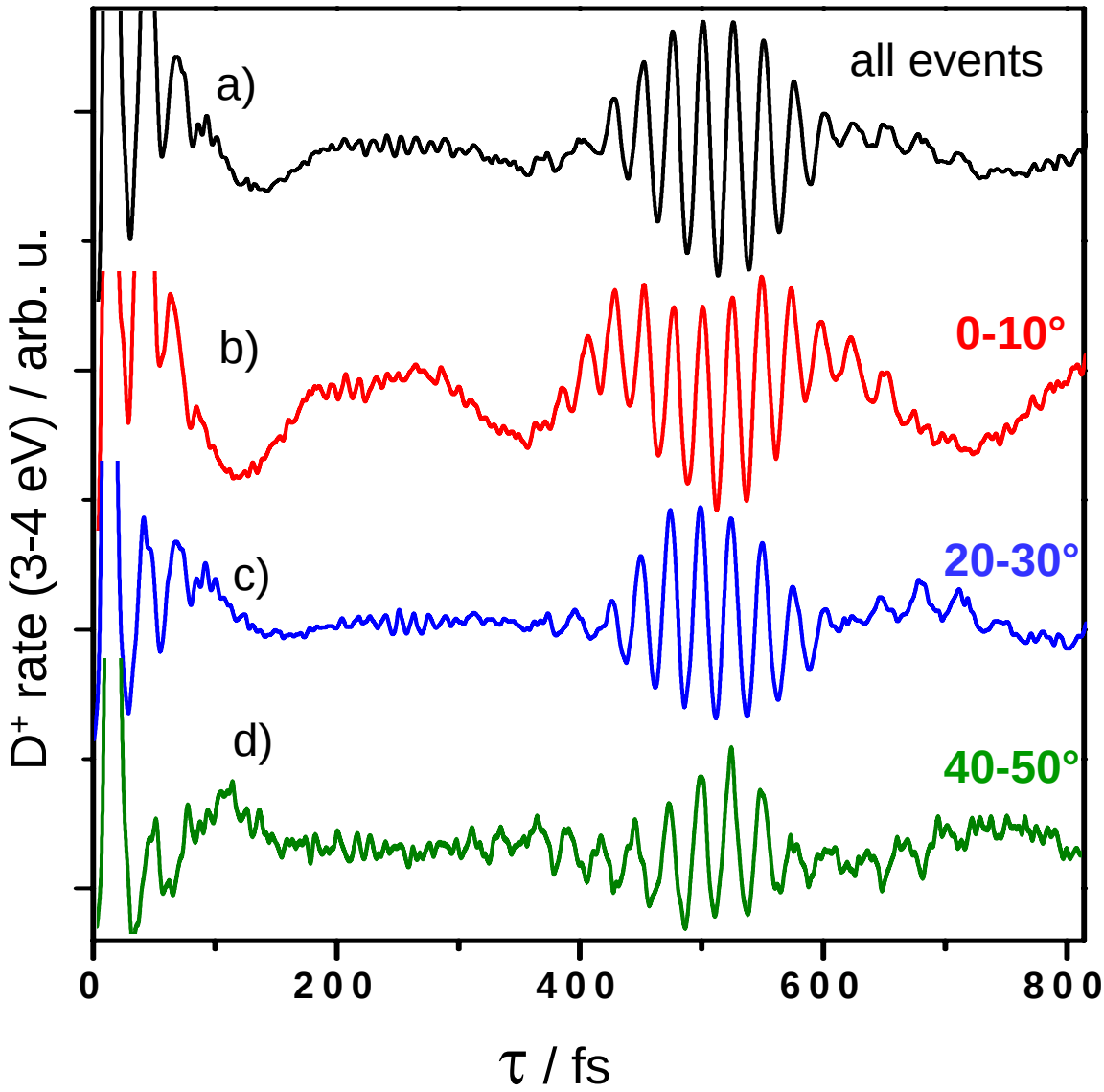
a)
all events
b)
0-10°
c)
20-30°
d)
40-50°
D+ rate (3-4 eV) / arb. u.
0
200
400
600
800
τ / fs

Figure 3

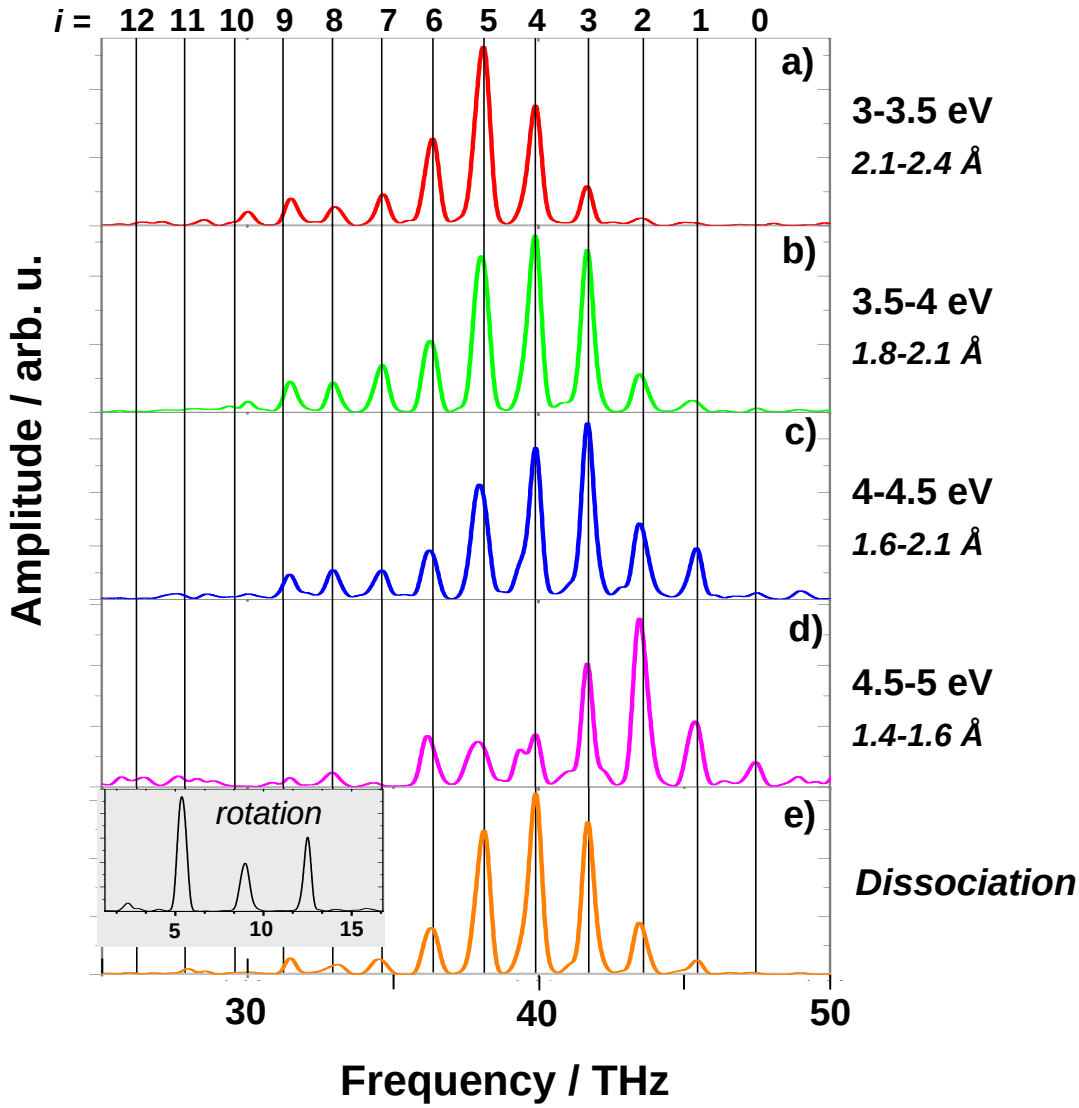
i = 12 11 10 9 8 7 6 5 4 3 2 1 0
a)
3-3.5 eV
2.1-2.4 Å
b)
3.5-4 eV
1.8-2.1 Å
c)
4-4.5 eV
1.6-2.1 Å
d)
4.5-5 eV
1.4-1.6 Å
e)
Dissociation
rotation
5
10
15
Amplitude / arb. u.
30
40
50
Frequency / THz

Figure 4